Journal of Solid State Chemistry 181 (2008) 2864–2868

Contents lists available at ScienceDirect

Journal of Solid State Chemistry

journal homepage: www.elsevier.com/locate/jssc

Syntheses, crystal structures and Si solubilities of new layered carbides $Zr_2Al_4C_5$ and $Zr_3Al_4C_6$

Keita Sugiura [a], Tomoyuki Iwata [a], Hideto Yoshida [b], Shinobu Hashimoto [a], Koichiro Fukuda [a,*]

[a] Department of Environmental and Materials Engineering, Nagoya Institute of Technology, Nagoya 466-8555, Japan
[b] Department of Earth and Planetary Science, Graduate School of Science, The University of Tokyo, Tokyo 113-0033, Japan

ARTICLE INFO

Article history:
Received 25 February 2008
Received in revised form
7 July 2008
Accepted 13 July 2008
Available online 22 July 2008

Keywords:
Layered carbides
Solid solutions
Powder diffraction
Rietveld refinement

ABSTRACT

Two types of new ternary carbides, $Zr_2Al_4C_5$ and $Zr_3Al_4C_6$, have been synthesized and characterized by X-ray powder diffraction. The crystal structures were refined from laboratory X-ray powder diffraction data ($CuK\alpha_1$) using the Rietveld method. These carbides form a homologous series with the general formula $(ZrC)_mAl_4C_3$ ($m=2$ and 3). The crystal structures can be regarded as intergrowth structures where the Al_4C_3-type $[Al_4C_4]$ layers are the same, while the NaCl-type $[Zr_mC_{m+1}]$ layers increase in thickness with increasing m value. The new carbides are most probably the end members of continuous solid-solutions $(ZrC)_m[Al_{4-x}Si_x]C_3$ with $0 \leqslant x \leqslant 0.44$.

1. Introduction

In the system Zr–Al–C, two types of ternary carbides have been confirmed so far: $Zr_2Al_3C_4$ and $Zr_3Al_3C_5$ [1,2]. These compounds form a homologous series, the general formula of which is $(ZrC)_nAl_3C_2$ ($n=2$ and 3) [1]. The crystal structures, belonging to the same space group $P6_3mc$, can be regarded as intergrowth structures where the Al_4C_3-type $[Al_3C_3]$ layers are the same, while the NaCl-type $[Zr_nC_{n+1}]$ layers increase in thickness with increasing n value. These two types of layers share the carbon-atom network at their boundaries; the C–C distances are ~0.335 nm for both carbides with $n=2$ and 3. On the other hand, the C–C distance of the ZrC crystal is 0.330 nm ($=a(ZrC)/\sqrt{2}$) and that of Al_4C_3 is 0.334 nm ($=a(Al_4C_3)$), where $a(ZrC)$ and $a(Al_4C_3)$ represent the a-axis lengths of the ZrC and Al_4C_3 crystals, respectively. These distances are close to each other, and also to those of the carbon-atom networks in $(ZrC)_nAl_3C_2$. Fukuda et al. have therefore concluded that the closeness of the C–C distances between the ZrC and Al_4C_3 crystals, being expressed by the equation $a(ZrC)/\sqrt{2} \approx a(Al_4C_3)$, is the principal reason for the formation of these layered carbides [1].

In the quaternary system Zr–Al–Si–C, new carbides $Zr_2[Al_{3.56}Si_{0.44}]C_5$ [3] and $Zr_3[Al_{3.56}Si_{0.44}]C_6$ [4] have been recently recognized. They also form a homologous series with the general formula $(ZrC)_n[Al_{3.56}Si_{0.44}]C_3$ ($n=2$ and 3). These crystal structures (space group $R3m$) can be regarded as intergrowth structures consisting of the Al_4C_3-type $[Al_{3.56}Si_{0.44}C_4]$ layers separated by the NaCl-type $[Zr_nC_{n+1}]$ layers.

From analogy with the existence of the homologous carbides $(ZrC)_nAl_3C_2$, we have expected the formation of new layered carbides for the reaction products ZrC and Al_4C_3. In the present study, we have experimentally confirmed the existence of a new homologous series comparable to $(ZrC)_n[Al_{3.56}Si_{0.44}]C_3$ ($n=2$ and 3) in the Zr–Al–C system. The crystal structures have been refined from XRPD data using direct methods, and described in relation to those of ZrC, Al_4C_3, $(ZrC)_nAl_3C_2$ and $(ZrC)_n[Al_{3.56}Si_{0.44}]C_3$.

2. Experimental

2.1. Syntheses of new carbides

The two types of new ternary carbides were initially recognized as unidentifiable diffraction lines in the XRPD patterns of the reacted ZrC–Al_4C_3 mixtures. The XRPD patterns of these carbides were almost identical to those of either $(ZrC)_2[Al_{3.56}Si_{0.44}]C_3$ or $(ZrC)_3[Al_{3.56}Si_{0.44}]C_3$. Since the present specimens were free from the Si component, the new carbides must be $(ZrC)_2Al_4C_3$ and $(ZrC)_3Al_4C_3$. We obtained by the following procedures the two types of powder samples: one consisted mainly of $(ZrC)_2Al_4C_3$ (sample S-A) and the other was mainly composed of $(ZrC)_3Al_4C_3$ (S-B).

The reagent-grade chemicals of ZrC (99.9%, KCL Co., Ltd., Saitama, Japan) and Al_4C_3 (KCL, 99.9%) were mixed in two

* Corresponding author. Fax: +81 52 735 5289.
E-mail address: fukuda.koichiro@nitech.ac.jp (K. Fukuda).

0022-4596/$ - see front matter © 2008 Elsevier Inc. All rights reserved.
doi:10.1016/j.jssc.2008.07.017

different molar ratios of $[ZrC:Al_4C_3] = [2:3]$ for S-A and $[ZrC:Al_4C_3] = [3:1]$ for S-B. Each of the well-mixed chemicals was pressed into pellets ($\varnothing$ 13 mm × 10 mm), heated at 2073 K for 1 h in inert gas atmosphere of Ar, followed by cooling to ambient temperature by cutting the furnace power. Both reaction products were slightly sintered polycrystalline materials. They were finely ground to obtain powder specimens. A small amount of Al_4C_3 crystallites coexisted in S-A, which was completely removed by dissolution with acid solution. In S-B, a relatively large amount of ZrC crystallites remained unreacted, which was caused by the preferential evaporation of the Al_4C_3 component during heating.

2.2. Flux growth of solid-solution crystals $(ZrC)_2[Al_{4-x}Si_x]C_3$

The reagent-grade chemicals of ZrC, Al (KCL, 99.9%), SiC (KCL, 99.9%) and C (graphite, KCL, 99.9%) were mixed in molar ratios of $[ZrC:Al:SiC:C] = [9:45:2:7]$. The well-mixed chemicals were pressed into pellets ($\varnothing$ 13 mm × 10 mm), heated at 1973 K for 1 h in inert Ar gas atmosphere, followed by cooling to ambient temperature by cutting the furnace power. The carbide crystals developed in the presence of liquid Al. The residual Al (metal state at ambient temperature) was completely removed by dissolution with acid solution. The resulting specimen was a slightly sintered polycrystalline material, mainly consisting of $(ZrC)_2[Al_{4-x}Si_x]C_3$ solid-solution crystals together with a very small amount of $(ZrC)_2Al_3C_2$.

2.3. Characterization

XRPD intensities of the powder specimens were collected on a diffractometer (X'Pert PRO Alpha-1, PANalytical B.V., Almelo, The Netherlands) equipped with a high-speed detector in the

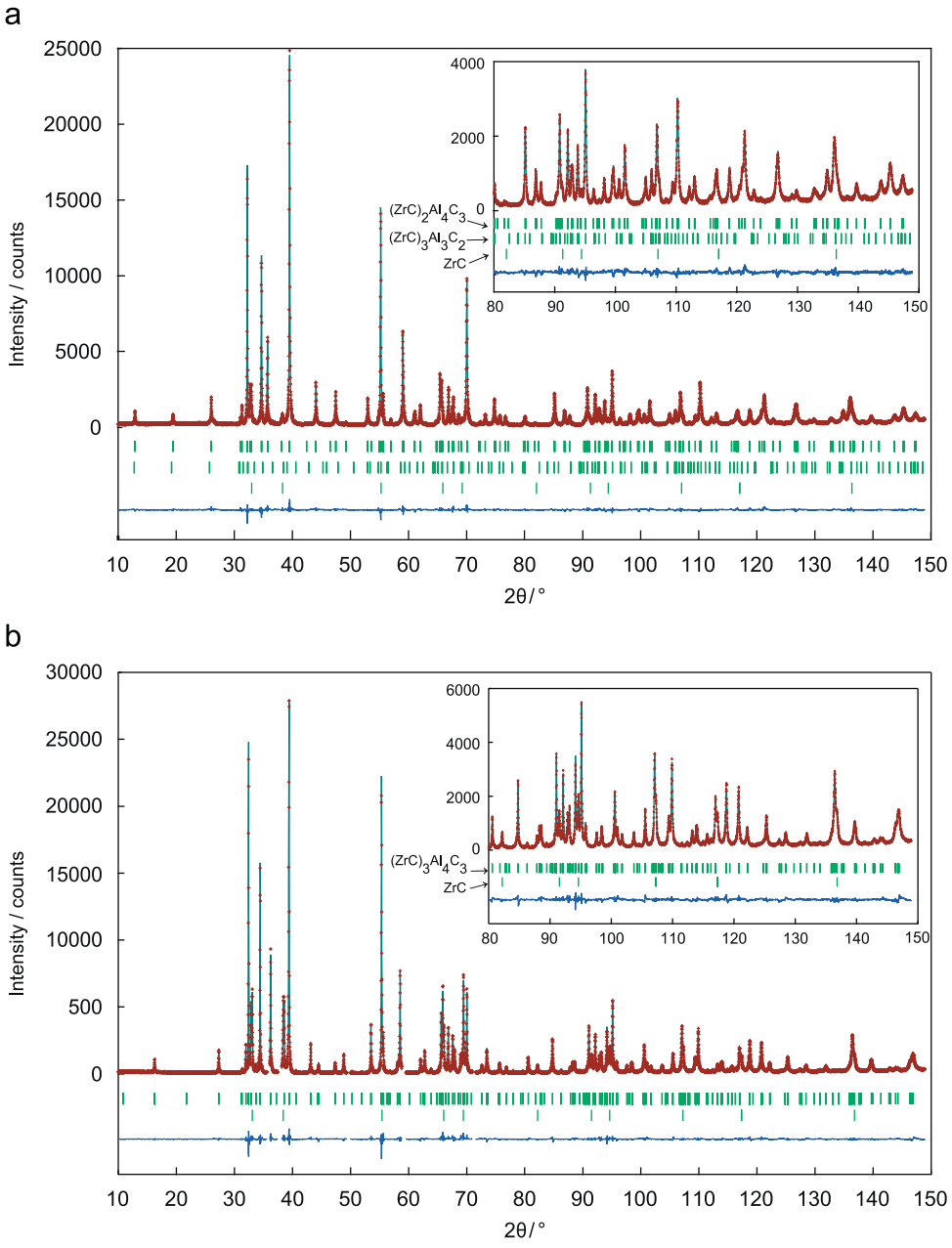

Fig. 1. Comparison of the observed diffraction patterns (symbol: +) with the corresponding calculated patterns (upper solid lines). The difference curves are shown in the lower part of the diagrams. Upper vertical bars in each diagram indicate the positions of possible Bragg reflections. The profile intensities for S-A in (a) and S-B in (b).

Bragg–Brentano geometry using monochromatized Cu$K\alpha_1$ radiation (45 kV, 40 mA) in a 2θ range from 10.0144° to 148.9017° (an accuracy in 2θ of $\pm$0.0001°). The automatic divergence slit was employed to maintain an illumination length of 5 mm on the sample. Thus, the quantitative profile intensities were collected over the whole 2θ range. Other experimental conditions were continuous scan, total of 8312 data points and total experimental time of 7.2 h. The structure data were standardized using the computer program STRUCTURE TIDY [5]. The crystal-structure models were visualized with the computer program VESTA [6].

The outer shape of the flux-grown crystals of $(ZrC)_2[Al_{4-x}Si_x]C_3$ were observed using a scanning electron microscope (SEM, JSM-6360, JEOL, Ltd., Tokyo, Japan). Polished section was prepared for the crystals and quantitative spot analysis was carried out to determine the chemical composition using an electron probe microanalyzer (EPMA, JCMA-733, JEOL). The correction for intensities was made using the ZAF routines. The standard materials used were synthetic $(ZrC)_2Al_3C_2$ (Zr and Al) and synthetic SiC (Si). The phase constitution was examined by XRPD.

3. Results and discussion

3.1. Structure refinement

Initial structural parameters of $(ZrC)_2Al_4C_3$ in S-A and $(ZrC)_3Al_4C_3$ in S-B were taken from those determined by Fukuda et al. for $(ZrC)_2[Al_{3.56}Si_{0.44}]C_3$ [3] and $(ZrC)_3[Al_{3.56}Si_{0.44}]C_3$ [4], respectively. The structural parameters were individually refined by the Rietveld method using the computer program RIETAN-FP [7]. The structure models of $(ZrC)_3Al_3C_2$ [2] and ZrC were added into the refinement as additional phases. A Legendre polynomial was fitted to background intensities with 12 adjustable parameters. The split Pearson VII function [8] was used to fit the peak profile. The isotropic atomic displacement parameters (B) of the Al sites were constrained to have the same value and those of the C sites as well. The reliability indices [9] for the final result of S-A were $R_{wp} = 6.29\%$, $S = 1.45$ and $R_p = 4.75\%$ ($R_B = 0.83\%$ and $R_F = 0.44\%$ for $(ZrC)_2Al_4C_3$) (Fig. 1(a)) and those of S-B were $R_{wp} = 7.94\%$, $S = 1.74$ and $R_p = 5.69\%$ ($R_B = 0.90\%$ and $R_F = 0.44\%$ for $(ZrC)_3Al_4C_3$) (Fig. 1(b)). The crystal data and the final atomic positional and B parameters of $(ZrC)_2Al_4C_3$ are, respectively, given in Tables 1 and 2, and those of $(ZrC)_3Al_4C_3$ in Tables 3 and 4. The selected interatomic distances, together with their standard deviations, are given in Tables 5 and 6. Quantitative X-ray analysis with correction for microabsorption according to Brindley's procedure [10] was implemented in the program RIETAN-FP. The phase compositions were found to be 94.7 mass% $(ZrC)_2Al_4C_3$, 1.8 mass% $(ZrC)_3Al_3C_2$ and 1.5 mass% ZrC for S-A and 85.5 mass% $(ZrC)_3Al_4C_3$ and 14.5 mass% ZrC for S-B.

3.2. Structure description

The new carbides $(ZrC)_2Al_4C_3$ and $(ZrC)_3Al_4C_3$ have been confirmed to be isostructural with $(ZrC)_2[Al_{3.56}Si_{0.44}]C_3$ and $(ZrC)_3[Al_{3.56}Si_{0.44}]C_3$, respectively. They form a homologous series with the general formula of $(ZrC)_mAl_4C_3$ ($m = 2$ and 3). The crystal structures may be regarded as intergrowth structures, which consist of the NaCl-type $[Zr_mC_{m+1}]$ layers (thickness of ~0.56 nm for $m = 2$ and ~0.82 nm for $m = 3$) separated by the Al_4C_3-type $[Al_4C_4]$ layers with ~0.81 nm thickness (Fig. 2). These two types of layers share the two-dimensional networks of carbon atoms at their boundaries; the C–C distances are 0.3322 nm for $m = 2$ and 0.3318 nm for $m = 3$. These values are close to each other, and also to the C–C distances of the networks in $(ZrC)_nAl_3C_2$.

The mean interatomic distances in $(ZrC)_mAl_4C_3$ compare well with those of ZrC, Al_4C_3, $(ZrC)_nAl_3C_2$ and $(ZrC)_n[Al_{3.56}Si_{0.44}]C_3$. The Zr sites are octahedrally coordinated by C atoms with the mean distances of 0.237 nm for $m = 2$ and 0.236 nm for $m = 3$, which are comparable to those of the ZrC_8 polyhedra in ZrC (0.235 nm), $(ZrC)_2Al_3C_2$ (0.241 nm), $(ZrC)_3Al_3C_2$ (0.239 nm), $(ZrC)_2[Al_{3.56}Si_{0.44}]C_3$ (0.238 nm) and $(ZrC)_3[Al_{3.56}Si_{0.44}]C_3$ (0.236 nm). The mean Zr–Al distances of 0.299 nm for $m = 2$ and 0.302 nm for $m = 3$ are comparable to the Zr–Al/Si distances of

Table 1
Crystal data for $(ZrC)_2Al_4C_3$

Chemical composition	$Zr_2Al_4C_5$
Space group	$R3m$
a (nm)	0.332169(3)
c (nm)	4.09479(3)
V (nm^3)	0.391274(5)
Z	3
D_x (Mg m^{-3})	4.46

Table 2
Structural parameters for $(ZrC)_2Al_4C_3$

Site	Wyckoff position	x	y	z	$100 \times B$ (nm^2)
Zr1	3a	0	0	0.6298(3)	0.49(3)
Zr2	3a	0	0	0.8984(3)	0.46(3)
Al1	3a	0	0	0.0696(3)	0.90(2)
Al2	3a	0	0	0.1752(4)	0.90
Al3	3a	0	0	0.3520(4)	0.90
Al4	3a	0	0	0.4502(3)	0.90
C1[a]	3a	0	0	0	0.38(5)
C2	3a	0	0	0.1283(5)	0.38
C3	3a	0	0	0.2660(4)	0.38
C4	3a	0	0	0.3993(6)	0.38
C5	3a	0	0	0.5303(1)	0.38

[a] z of C1 atom is fixed.

Table 3
Crystal data for $(ZrC)_3Al_4C_3$

Chemical composition	$Zr_3Al_4C_6$
Space group	$R3m$
a (nm)	0.331807(2)
c (nm)	4.89771(3)
V (nm^3)	0.466975(4)
Z	3
D_x (Mg m^{-3})	4.84

Table 4
Structural parameters for $(ZrC)_3Al_4C_3$

Site	Wyckoff position	x	y	z	$100 \times B$(nm^2)
Zr1	3a	0	0	0.3047(8)	0.38(1)
Zr2	3a	0	0	0.6925(9)	0.45(5)
Zr3	3a	0	0	0.9173(9)	0.63(6)
Al1	3a	0	0	0.0731(9)	1.08(4)
Al2	3a	0	0	0.1545(9)	1.08
Al3	3a	0	0	0.4474(9)	1.08
Al4	3a	0	0	0.5362(9)	1.08
C1[a]	3a	0	0	0	0.62(8)
C2	3a	0	0	0.1120(12)	0.62
C3	3a	0	0	0.2194(8)	0.62
C4	3a	0	0	0.3871(7)	0.62
C5	3a	0	0	0.4976(12)	0.62
C6	3a	0	0	0.6091(3)	0.62

[a] z of C1 atom is fixed.

Table 5
Interatomic distances (nm) in $(ZrC)_2Al_4C_3$[a]

Zr1–C3	0.2288(8) × 3
Zr1–C1	0.2442(8) × 3
Zr1–Al3	0.2975(5) × 3
Zr1–Zr2	0.32714(8) × 3
Zr2–C5	0.2387(8) × 3
Zr2–C3	0.2376(9) × 3
Zr2–Al2	0.3004(6) × 3
Al1–C4	0.1924(1) × 3
Al1–C2	0.2402(20)
Al1–Al4	0.2725(3) × 3
Al1–C1	0.2851(14)
Al1–Al3	0.2836(6) × 3
Al2–C2	0.1921(23)
Al2–C5	0.2115(7) × 3
Al2–Al4	0.3063(6) × 3
Al3–C1	0.2064(6) × 3
Al3–C4	0.1939(22)
Al4–C2	0.1974(4) × 3
Al4–C4	0.2086(21)
Al4–C5	0.3279(13)

[a] All distances shorter than 0.33 nm (metal–metal) and 0.33 nm (metal–carbon) are given.

Table 6
Interatomic distances (nm) in $(ZrC)_3Al_4C_3$[a]

Zr1–C1	0.2374(25) × 3
Zr1–C6	0.2384(23) × 3
Zr1–Zr3	0.3269(2) × 3
Zr1–Zr2	0.3282(2) × 3
Zr2–C1	0.2295(24) × 3
Zr2–C4	0.2356(13) × 3
Zr2–Al1	0.3007(9) × 3
Zr3–C6	0.2277(22) × 3
Zr3–C3	0.2450(14) × 3
Zr3–Al4	0.3025(8) × 3
Al1–C2	0.1905(33)
Al1–C4	0.2137(10) × 3
Al1–Al3	0.2772(9) × 3
Al2–C5	0.1974(8) × 3
Al2–C2	0.2081(31)
Al2–Al3	0.2757(5) × 3
Al2–Al4	0.3045(9) × 3
Al2–C3	0.3180(26)
Al3–C2	0.1918(1) × 3
Al3–C5	0.2459(36)
Al3–C4	0.2949(24)
Al4–C5	0.1891(35)
Al4–C3	0.2081(9) × 3

[a] All distances shorter than 0.33 nm (metal–metal) and 0.32 nm (metal–carbon) are given.

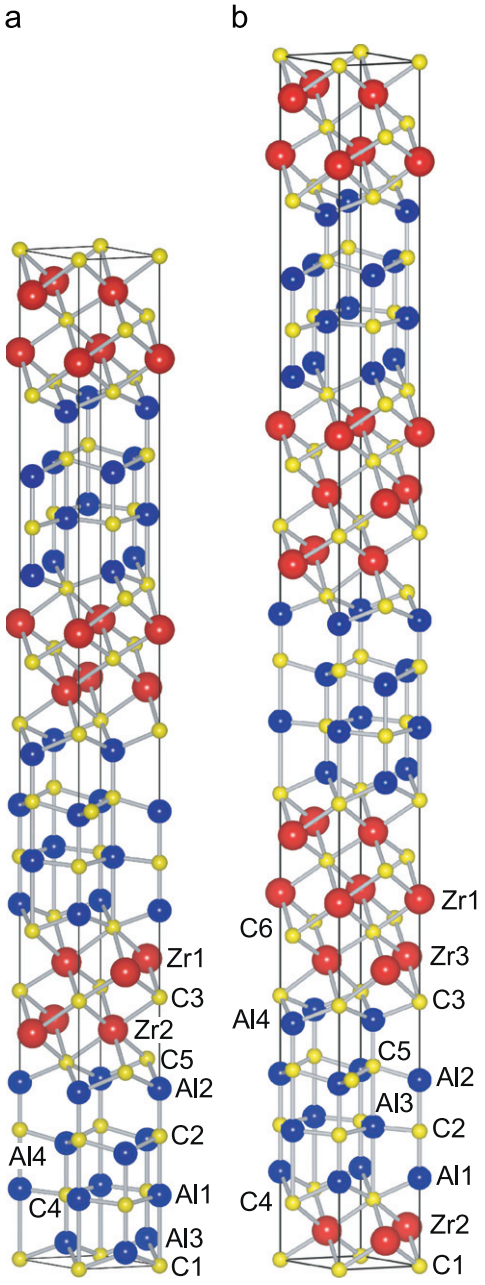

Fig. 2. Crystal structures of $(ZrC)_2Al_4C_3$ in (a) and $(ZrC)_3Al_4C_3$ in (b).

$(ZrC)_2Al_3C_2$ (0.297 nm), $(ZrC)_3Al_3C_2$ (0.297 nm), $(ZrC)_2[Al_{3.56}Si_{0.44}]C_3$ (0.299 nm) and $(ZrC)_3[Al_{3.56}Si_{0.44}]C_3$ (0.305 nm). The Al atoms are tetrahedrally coordinated with the mean distances of 0.203 nm for $m = 2$ and 0.204 nm for $m = 3$. These Al–C distances are comparable to those of the AlC_4 tetrahedra in Al_4C_3, ranging from 0.194 to 0.218 nm (the mean = 0.206 nm) [11], which implies that the $[Al_4C_4]$ layers of both $m = 2$ and 3 are structurally comparable to the compound Al_4C_3.

3.3. Chemical variation of $(ZrC)_2[Al_{4-x}Si_x]C_3$ solid solution

The outer shape of the flux-grown crystals showed hexagonal plates with the size up to 50 μm in diameter and about 10 μm in thickness (Fig. 3). The XRPD pattern was nearly identical to that of $(ZrC)_2[Al_{3.56}Si_{0.44}]C_3$. Based on the mass percentages of Zr, Al, Si and C determined by EPMA, the atomic ratios were derived on the basis of two zircon atoms in one formula unit as [Zr:Al:Si:C] = [2:3.76(5):0.09(6):4.33(8)]. The atomic ratios of the individual crystals examined were plotted with Al as the ordinate and Si as the abscissa (Fig. 4) and showed the following excellent correlation (correlation coefficient $r = 0.963$): Al = 3.853(7)−0.96(7) × Si where the figures in parentheses indicate standard deviations. This equation indicates that the Si atoms would exclusively go to the Al sites, with the sum total of Al and Si atoms being 4. Thus, the compound may be represented by the chemical formula $(ZrC)_2[Al_{4-x}Si_x]C_3$; the spot analysis of each crystal grain indicated that the x-value varied from 0.063 to 0.196. Accordingly, the new carbide $(ZrC)_2Al_4C_3$ ($x = 0$) is most probably the end member of continuous solid-solution $(ZrC)_2[Al_{4-x}Si_x]C_3$. The maximum x-value confirmed so far is 0.44 according to the

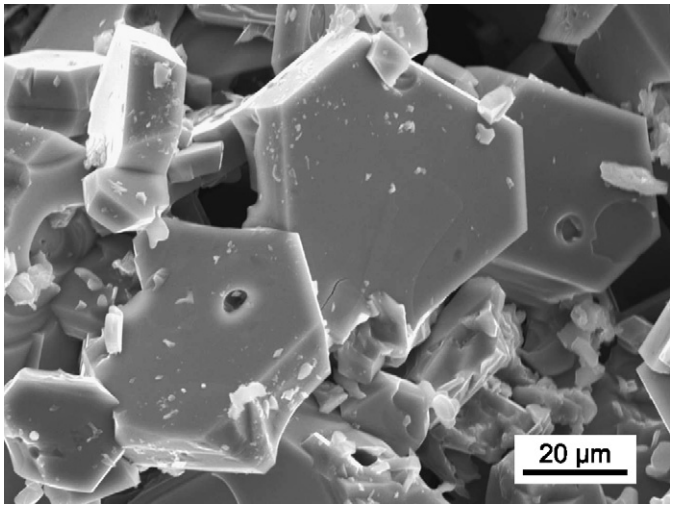

Fig. 3. SEM photograph of the flux-grown crystals of $(ZrC)_2[Al_{4-x}Si_x]C_3$ $(0.063 \leqslant x \leqslant 0.196)$.

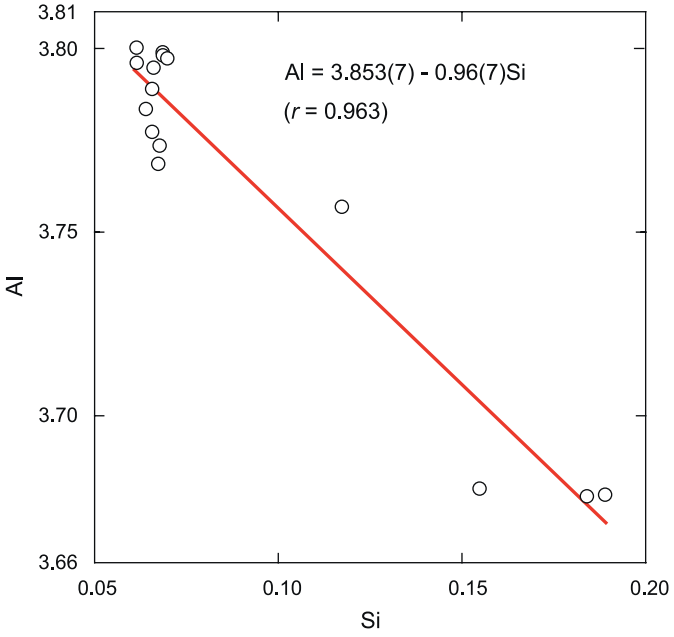

Fig. 4. Al versus Si variation diagram for the flux-grown crystals of $(ZrC)_2[Al_{4-x}Si_x]C_3$ $(0.063 \leqslant x \leqslant 0.196)$. The linear fit suggests Al+Si = 4.

previous study [3]. In the same manner as above, the other new carbide $(ZrC)_3Al_4C_3$ would be also the end member of the continuous solid-solution $(ZrC)_3[Al_{4-y}Si_y]C_3$ $(0 \leqslant y \leqslant 0.44)$.

4. Conclusion

In the Zr–Al–C system, we have successfully synthesized the two types of new carbides $(ZrC)_2Al_4C_3$ and $(ZrC)_3Al_4C_3$. The crystal structures were determined from XRPD data and described in relation to those of ZrC, Al_4C_3, $(ZrC)_2Al_3C_2$ and $(ZrC)_3Al_3C_2$. The crystal structures were considered to be composed of the NaCl-type $[Zr_mC_{m+1}]$ slabs separated by the Al_4C_3-type $[Al_4C_4]$ layers. Hence, they form a homologous series with the general formula $(ZrC)_mAl_4C_3$ ($m = 2$ and 3). The new carbides are most probably the end members of continuous solid-solutions $(ZrC)_m[Al_{4-x}Si_x]C_3$ $(0 \leqslant x \leqslant 0.44)$.

Acknowledgments

Thanks are due to Mr. T. Aoki, Nagoya Institute of Technology, for technical assistance. Supported by a Grant-in-Aid for Scientific Research (no. 18560654) from the Japan Society for the Promotion of Science.

References

[1] K. Fukuda, S. Mori, S. Hashimoto, J. Am. Ceram. Soc. 88 (2005) 3528–3530.
[2] Th.M. Gesing, W. Jeitschko, J. Solid State Chem. 140 (1998) 396–401.
[3] K. Fukuda, M. Hisamura, T. Iwata, N. Tera, K. Sato, J. Solid State Chem. 180 (2007) 1809–1815.
[4] K. Fukuda, M. Hisamura, Y. Kawamoto, T. Iwata, J. Mater. Res. 22 (2007) 2888–2894.
[5] L.M. Gelato, E. Parthé, J. Appl. Crystallogr. 20 (1987) 139–143.
[6] F. Izumi, K. Momma, Solid State Phenom. 130 (2007) 15–20.
[7] F. Izumi, T. Ikeda, Mater. Sci. Forum 321–324 (2000) 198–203.
[8] H. Toraya, J. Appl. Crystallogr. 23 (1990) 485–491.
[9] R.A. Young, in: R.A. Young (Ed.), The Rietveld Method, Oxford University Press, Oxford, UK, 1993, pp. 1–38.
[10] G.W. Brindley, Bull. Soc. Chim. France (1949) D59–D63.
[11] Th.M. Gesing, W. Jeitschko, Z. Naturforsch. B 50 (1995) 196–200.